Dalton Transactions

ROYAL SOCIETY OF CHEMISTRY

COMMUNICATION

View Article Online
View Journal | View Issue

Cite this: *Dalton Trans.*, 2025, **54**, 15020

Received 5th September 2025,
Accepted 8th September 2025

DOI: 10.1039/d5dt02134k

rsc.li/dalton

Phosphaza-norbornanes

Joseph Nazak,[a] Michael A. Land,[a,b] Jason D. Masuda[c] and Saurabh S. Chitnis*[a,d]

The first definitive isolation of phosphaza-norbornanes is reported. These PN frameworks feature a bicyclo[2.2.1]heptane skeleton with bridgehead P(III) sites and can be made *via* a modular condensation reaction starting from primary amines. Their molecular and electronic structures, stability, and strain energies are compared with closely related PN or hydrocarbon bicyclic systems.

The stability of C–C/H bonds and the long history of reaction development in organic chemistry allow a stunning diversity of skeletal motifs to be rationally targeted. Nevertheless, quantitative analyses of the Chemical Abstract Service show that hydrocarbon chains and rings are the dominant structures at the core of organic compounds.[1,2] By comparison, three-dimensional cages are rare due to (i) the accumulation of ring strain, and (ii) the reliance upon challenging ring-closures for accessing bicycles.[3,4] These synthetic limitations are also reflected in the paucity of such structures in applied contexts. Indeed, there is increasing recognition that an "escape from flatland"[5] holds great promise for medicinal[5,6] and materials chemistry,[4,7–11] motivating significant synthetic efforts towards framework diversification into the third dimension.[12–21]

The longer, more ionic, and more polarizable bonds of the inorganic elements engender less strain in closed structures than is the case for hydrocarbons.[22,23] Moreover, intermolecular condensations, instead of intramolecular ring-closures, can be used to assemble inorganic cages, allowing rapid variation.[22,23] As a result, the cage-dense parameter space in molecular and macromolecular chemistry is easier to explore using inorganic elements compared to hydrocarbons. As shown by the success of materials based on carboranes and polyhedral oligomeric silsesquioxanes (POSS), small inorganic cages are also valued as synthons due to their ability to enhance the thermal stability and mechanical properties of macromolecules.[24–30]

We are interested in the phosphaza (PN) cages first reported by Holmes, Nöth, and Payne in the 1970s (Fig. 1).[31,32] The PN-bicyclo[2.2.2]octane (**A**) or PN-adamantane (**B**), featuring a P_2N_6 or P_4N_6 skeleton, respectively, can be synthesized in near-quantitative yields on multigram scales *via* solution or solid-phase condensation between commodity amines or hydrazines and P(III) electrophiles.[33–35] We have shown that their oxidation to **C** and **D** yields masked polynucleophiles with P_2N_8 or P_4N_{10} compositions.[36–38] Cages **A–D** can also be modularly combined with diazides or dihalides to make a rapidly evolving family of inorganic polymers and materials.[7,33,36,37,39,40] Besides being potential synthons for useful functional materials, the development of new P_xN_y skeletons is also fundamentally important in terms of expanding the known diversity of inorganic scaffolds.

Here we reveal the modular synthesis, structures, and electronic features of PN-norbornanes having a P_2N_5 skeleton, pro-

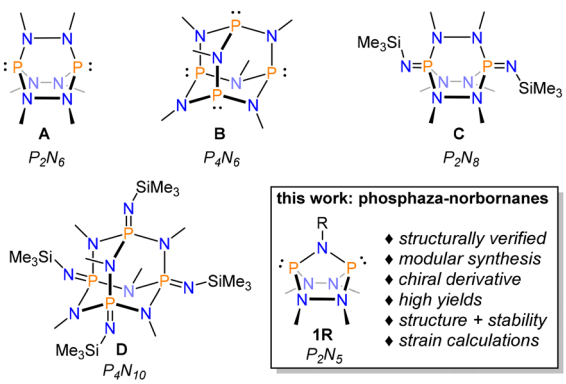

Fig. 1 PN cages **A–D** and the phosphaza-norbornanes **1R** reported here. Formulae in italics denote skeletal composition in terms of phosphorus–nitrogen ratios.

[a]*Department of Chemistry, Dalhousie University, 6241 Alumni Crescent, Halifax, Nova Scotia, B3H 4R2, Canada. E-mail: chitnis@uvic.ca*
[b]*Department of Chemistry and Physics, Mount Saint Vincent University, Halifax, Nova Scotia, B3M 2J6, Canada*
[c]*Department of Chemistry, Saint Mary's University, 923 Robie Street, Halifax, Nova Scotia, B3H 3C3, Canada*
[d]*Department of Chemistry, University of Victoria, Victoria, British Columbia, V8B 5C2, Canada*

viding fundamental comparative insights, and setting the stage for future applied developments with a highly-tunable new PN cage.

Our approach was initially guided by Nöth's claim that dichloride ring **E** reacts with $MeN(SiMe_3)_2$ to form **1Me**, but only NMR data, melting point, and elemental analysis were reported for the product, and no structural verification was made, nor was any other derivative accessed.[41] We found that the reaction of **E** with bis-silylamines indeed proceeds with Me_3SiCl loss and formation of compounds **1R**, but the scope of this reaction was severely limited (Fig. 2). Due to the considerable steric hindrance imposed by the $SiMe_3$ group, Me_3SiCl condensation is only operative for unhindered alkylamines and moreover first requires the synthesis of the precursor bis-silylamines. Attempts to convert the prototypical **1Me** to other derivatives *via* amine metathesis in the presence of excess primary amines at elevated temperatures were unsuccessful.

Instead, dehydrochlorination between ring **E** and a wide range of primary amines in the presence of excess NEt_3 cleanly yielded derivatives of **1R** in excellent spectroscopic yields, and good isolated yields (60–89%), directly from the commercial amines. The compounds show a sharp signal in the δ = 80–100 ppm range in their ^{31}P NMR spectrum, which is shifted significantly upfield of the signal for **E** (120 ppm). The reaction shows a wide scope with aliphatic, aromatic, allylic, pyridyl and fluorinated amines being viable for incorporation into the respective phosphaza-norbornanes. For example, the use of a diamine enabled formation of doubly-cage functionalized compound **1tmb**, and the use of an amino-acid ester gave the chiral compound **1Phe**. Notably, while the two dimethylhydrazino arms in all other derivatives are equivalent by ^1H NMR spectroscopy, those in **1Phe** are expectedly diastereotopic due to a stereogenic benzyl carbon.

X-ray diffraction experiments on single crystals of **1Mes**, **1ArF**, and **1tmb** provided definitive structural authentication for PN-norbornanes (Fig. 3, see also Table S1, SI). For comparison, the structure for **A** was also reobtained at 150 K, as the previously reported data at 298 K was not suitable beyond connectivity discussion.[42] All compounds show a folded rectangle structure for the P_2N_4 portion, with N-Me groups being staggered to avoid an eclipsed arrangement. There are three significant structural consequences of the short single nitrogen bridge in derivatives of **1R**. First, the P1···P2 separation involving the bridgehead positions is much smaller (*ca.* 2.7 Å) than the value in **A** [*ca.* 3.011(4) Å]. Second, the P1/2–N3 bond length involving the bridging nitrogen are elongated by *ca.* 0.06 Å relative to all other P–N bond lengths. And finally, the bridging P1–N3–P2 bond angles lie in the 102.69(18)°–103.22(12)° range, whereas the remaining N–P–N bond angles in derivatives of **1R** [90.84(16)°–99.64(8)°] are smaller compared to those in **A** [97.38 (18)°–104.3(3)°]. The only intermolecular contacts observed in the lattice of **1Mes** and **1tmb** are between the methyl groups, likely resulting from weak dispersion interactions. In the case of **1ArF**, long C···F contacts (3.11 Å) involving the C_6F_5 groups are observed, which are only slightly smaller than the sum of the van der Waals radii for the two elements (3.17 Å). The minimal intermolecular interaction is consistent with the excellent solubility of PN-norbornanes in hydrocarbon solvents, the sub-room temperature melting points when R is an alkyl group, and low melting points even for aryl derivatives (*e.g.* 40–41 °C for **1ArF**, and 63–65 °C for **1Mes**).

Stability tests involving exposure to heat, UV irradiation, and humid air were conducted with **1Me**, **1Ph**, and **1ArF** and

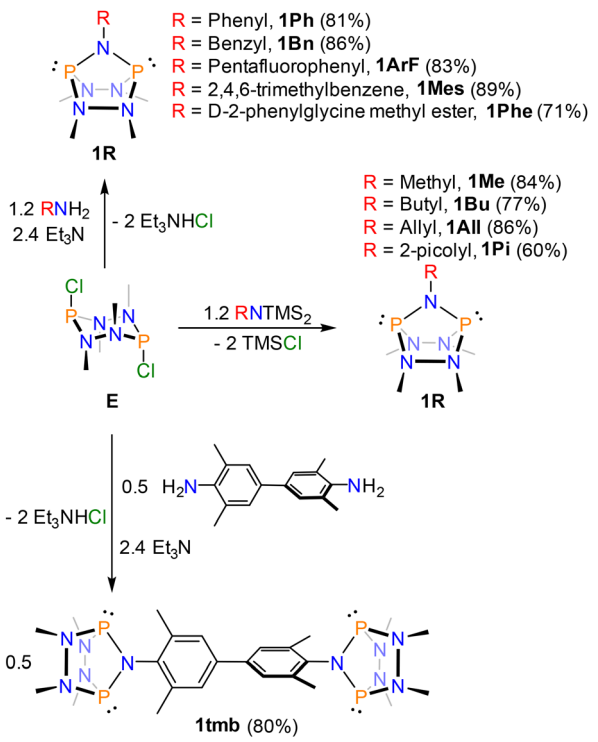

Fig. 2 Synthesis and scope of **1R**.

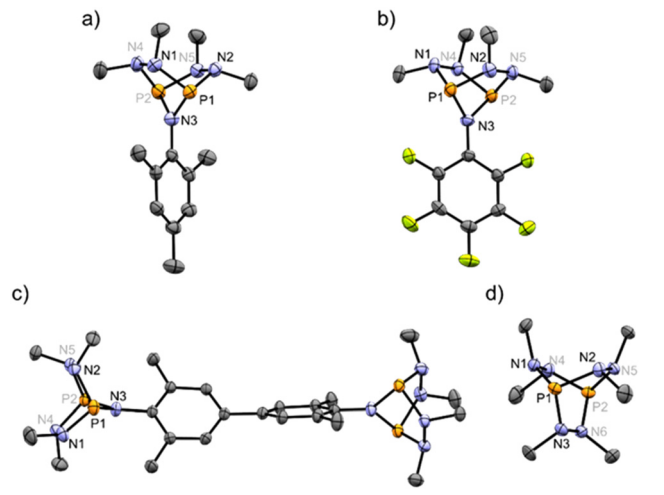

Fig. 3 Structures of (a) **1Mes**, (b) **1ArF**, (c) **1tmb**, and (d) **A** in the solid state. Hydrogen atoms are omitted for clarity. Ellipsoids are shown at the 50% probability level.

A. All derivatives showed excellent thermal and UV stability in dry THF, with <10% degradation after 48 h. However, the PN-norbornanes degraded almost completely to a complex mixture of P(v) species [*e.g.* phosphine oxides, $\delta(^{31}P) = -5$ to +10 ppm] within 2 hours of exposure to ambient air (80% humidity) as THF solutions (Fig. S2–S7). In the case of **1ArF**, the free aniline $C_6F_5NH_2$ was detected as the major product, consistent with hydrolytic removal of the NC_6F_5 group. In sharp contrast, a THF solution of **A** showed <2% degradation in air over this period (Fig. S8), indicating its air stability. Thus, PN-norbornanes **1R** show greater reactivity towards oxidants and moisture compared with PN-bicyclooctane **A**, and we hypothesized this may be due to intrinsic differences between the lone pair energies and/or the relative bicyclic strain in the two systems. These factors are sequentially discussed below.

Fig. 4a shows the molecular orbital identifiable as having significant P(III) lone pair character for **1Me** and **A**. In both cases, this is HOMO−3, while HOMO, HOMO−1, and HOMO−2 are derived from combinations of nitrogen lone pairs (see Fig. S60). Due to geometric constraints, the P(III) lone pairs are more accessible than the higher energy nitrogen lone pairs.[44] Comparison of the HOMO−3 energies for **1Me** (−6.25 eV) and **A** (−6.24 eV) indicates that the P(III) lone pairs in these frameworks are essentially equivalent in their intrinsic basicity, albeit the ones in the PN-norbornane are more spatially diffuse and accessible. The calculated lone pair MO energies for **1Me** (−6.25 eV), **1Ph** (−6.25 eV) and **1ArF** (−6.53 eV) indicates that within the PN-norbornanes, P(III) basicity does not change upon substitution of N-Me with an N-Ph group but does decrease considerably upon introduction of the N-C_6F_5 group.

The electron localization function (ELF), which has a range between 0 and 1, with larger values indicating more strongly localized electrons, provides a complementary topological signature of lone pairs.[45] As shown in Fig. 4b, two strongly localized regions are observed at the phosphorus atoms in both **1Me** and **A**. However, due to the geometric constraint applied by the single nitrogen bridge, the lone pairs in the PN-norbornane are distorted towards N3 to form an angle of 137°, whereas those in the PN-bicyclooctane show a mutual angular separation of 180°. The spatial extent of the lone pairs in **1Me** is also noticeably greater, consistent with the MO picture. In the context of coordination chemistry, therefore, the two diphosphine frameworks can be viewed as being equally strong donors, but **A** features a linear and more sterically shielded arrangement of the two P(III) sites, while **1Me** is bent with more accessible P(III) lone pairs. These differences may explain the observed higher reactivity of **1R** relative to **A**.

To assess the role of strain in the higher reactivity of **1R** we used the homodesmotic scheme shown in Fig. 4c. This approach reveals the *relative* strain in the two frameworks due to the presence of either one- or two-atom long bridges. The calculations show (Table 1) that **1Me** is marginally more strained (*ca.* 4.5 kJ mol^{-1}) than **A**. Within the PN-norbornanes family, bridging *via* an N-Ph group rather than N-Me group reduces strain considerably such that **1Ph** shows a lower strain energy (4.3 kJ mol^{-1}) than even the larger framework **A** (14.0 kJ mol^{-1}). On the other hand, bridging *via* an electron-deficient N-C_6F_5 group increases ring strain in **1ArF** (21.3 kJ mol^{-1}). This agrees with the observations that (i) the experimental P1/2–N3 distance is greatest for **1ArF** amongst derivatives of **1R** (Table S1), and (ii) **1ArF** decomposes the fastest upon exposure to moisture. Thus, the greater strain in PN-norbornanes – particularly electron deficient-derivatives – also contributes to their greater reactivity compared to **A**. Importantly, the range of values calculated for the PN frameworks (4.3–21.3 kJ mol^{-1}) is significantly lower than those for hydrocarbon ones, and the differences between the two bicyclic frameworks are more pronounced for the hydrocarbon case. Thus, PN cages are not only less strained than organic ones, but also less sensitive to strain accumulation upon introduction of more severe bicyclic constraints. Nevertheless, the stark reactivity differences between **1R** and **A** are a reminder that small strain differences can be chemically consequential.

In summary, we debuted phosphaza-norbornanes as a new inorganic scaffold and used comparative analyses of molecular structure, stability, electronic structure, and strain to emphasize their distinct features relative to PN or carbon-based analogues. The modular polycondensation approach used to access **1R** is attractive as it permits extensive side-groups variation, as shown by incorporation even of a chiral amino-acid ester in **1Phe**. Such tunability is absent in **A** and very challen-

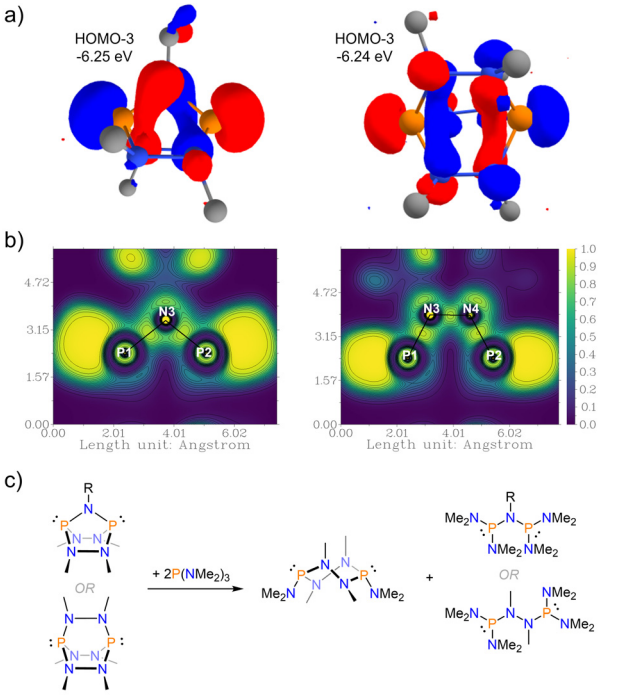

Fig. 4 (a) Visualization of the HOMO−3 for **1Me** (left) and **A** (right), representing one of two P(III) lone pair MOs. (b) Contour plots of the electron localization function (ELF) in the plane defined by P1–N3–P2 (**1Me**, left) and P1–N3–N4–P2 (**A**, right).[43] (c) Homodesmotic scheme used to determine relative strain in **1R** and **A**.

Table 1 Calculated strain energy (kJ mol^{-1}) imposed by the bicyclic constraints in **1R**, **A**, and relevant hydrocarbon systems, relative to six-membered PN or hydrocarbon rings

A[a]	**1Me**[a]	**1Ph**[a]	**1ArF**[a]	Norbornane[b]	Bicyclo[2.2.2]octane[b]
14.0	18.4	4.3	21.3	64.0 [60.2]	43.1 [31.0]

[a] Calculated using the r^{2}SCAN-3c composite method *via* the homodesmotic scheme shown in Fig. 4c. [b] Calculated using experimental values *via* homodesmotic scheme [RSE(bicycloalkane)–RSE(cyclohexane)].[46,47]

ging to implement in hydrocarbons. These results advance our fundamental understanding of structure and strain in inorganic frameworks, while providing a new axis for rapidly tuning the properties of a burgeoning class of P_xN_y cage-based materials.[7,33,36,37,39,40] Studies leveraging this framework variability are underway and will be reported in the future.

Conflicts of interest

There are no conflicts to declare.

Data availability

The data supporting this article have been included as part of the supplementary information (SI). Synthetic details, spectroscopic data and Cartesian coordinates of calculated structures. See DOI: **https://doi.org/10.1039/d5dt02134k**.

CCDC 2331623 and 2477097–2477099 contain the supplementary crystallographic data for this paper.[48a–d]

Acknowledgements

The Natural Sciences and Engineering Research Council of Canada (NSERC) is acknowledged by JN, SSC, MAL and JDM. SSC acknowledges the Alfred P Sloan Research Foundation for a Fellowship and the Dalhousie University Research Chairs program for support.

References

1 A. H. Lipkus, S. P. Watkins, K. Gengras, M. J. McBride and T. J. Wills, *J. Org. Chem.*, 2019, **84**, 13948–13956.
2 A. H. Lipkus, Q. Yuan, K. A. Lucas, S. A. Funk, W. F. Bartelt III, R. J. Schenck and A. J. Trippe, *J. Org. Chem.*, 2008, **73**, 4443–4451.
3 K. E. Prosser, R. W. Stokes and S. M. Cohen, *ACS Med. Chem. Lett.*, 2020, **11**, 1292–1298.
4 G. M. Locke, S. S. R. Bernhard and M. O. Senge, *Chem. – Eur. J.*, 2019, **25**, 4590–4647.
5 F. Lovering, J. Bikker and C. Humblet, *J. Med. Chem.*, 2009, **52**, 6752–6756.
6 F. Lovering, *MedChemComm*, 2013, **4**, 515–519.
7 J. Bedard and S. S. Chitnis, *Chem. Mater.*, 2023, **35**, 8338–8352.
8 N. T. Tsui, Y. Yang, A. D. Mulliken, L. Torun, M. C. Boyce, T. M. Swager and E. L. Thomas, *Polymer*, 2008, **49**, 4703–4712.
9 N. T. Tsui, A. J. Paraskos, L. Torun, T. M. Swager and E. L. Thomas, *Macromolecules*, 2006, **39**, 3350–3358.
10 X.-D. Hu, S. E. Jenkins, B. G. Min, M. B. Polk and S. Kumar, *Macromol. Mater. Eng.*, 2003, **288**, 823–843.
11 L. K. Macreadie, K. B. Idrees, C. S. Smoljan and O. K. Farha, *Angew. Chem., Int. Ed.*, 2023, **62**, e202304094.
12 D. Feng, X. Geng, L. Zuo, Z. Li and L. Wang, *Adv. Sci.*, 2025, **12**, 2501310.
13 H. F. Klein, D. J. Hamilton, I. J. P. de Esch, M. Wijtmans and P. O'Brien, *Drug Discovery Today*, 2022, **27**, 2484–2496.
14 B. Cox, V. Zdorichenko, P. B. Cox, K. I. Booker-Milburn, R. Paumier, L. D. Elliott, M. Robertson-Ralph and G. Bloomfield, *ACS Med. Chem. Lett.*, 2020, **11**, 1185–1190.
15 B. Cox, K. I. Booker-Milburn, L. D. Elliott, M. Robertson-Ralph and V. Zdorichenko, *ACS Med. Chem. Lett.*, 2019, **10**, 1512–1517.
16 N. V. Suryanarayana Birudukota, R. Franke and B. Hofer, *Org. Biomol. Chem.*, 2016, **14**, 3821–3837.
17 H. F. Reinhardt, *J. Polym. Sci., Part B: Polym. Lett.*, 1964, **2**, 567–568.
18 J. Friebel, C. P. Ender, M. Mezger, J. Michels, M. Wagner, K. B. Wagener and T. Weil, *Macromolecules*, 2019, **52**, 4483–4491.
19 Z. Chen and T. M. Swager, *Macromolecules*, 2008, **41**, 6880–6885.
20 E. Hoffmeister, J. E. Kropp, T. L. McDowell, R. H. Michel and W. L. Rippie, *J. Polym. Sci., Part A: Polym. Chem.*, 1969, **7**, 55–72.
21 F. Ishiwari, G. Okabe, T. Kajitani and T. Fukushima, *ACS Macro Lett.*, 2021, **10**, 1529–1534.
22 M. Veith, *Chem. Rev.*, 1990, **90**, 3–16.
23 N. Rinn, I. Rojas-Leon, B. Peerless, S. Gowrisankar, F. Ziese, N. W. Rosemann, W. C. Pilgrim, S. Sanna, P. R. Schreiner and S. Dehnen, *Chem. Sci.*, 2024, **15**, 9438–9509.
24 X. Zhang, L. M. Rendina and M. Müllner, *ACS Polym. Au.*, 2024, **4**, 7–33.
25 Y. Morisaki, in *Encyclopedia of Polymeric Nanomaterials*, ed. S. Kobayashi and K. Müllen, Springer Berlin Heidelberg, Berlin, Heidelberg, 2021, pp. 1–5. DOI: **10.1007/978-3-642-36199-9_123-1**.
26 M. Birot, J.-P. Pillot and J. Dunogues, *Chem. Rev.*, 1995, **95**, 1443–1477.
27 M. P. Maskarinec and G. Olerich, *Anal. Chem.*, 1980, **52**, 588–591.
28 E. Ayandele, B. Sarkar and P. Alexandridis, *Nanomaterials*, 2012, **2**, 445.
29 D. B. Cordes, P. D. Lickiss and F. Rataboul, *Chem. Rev.*, 2010, **110**, 2081–2173.
30 G. Li, L. Wang, H. Ni and C. U. Pittman, *J. Inorg. Organomet. Polym. Mater.*, 2001, **11**, 123–154.

31 R. B. Holmes and J. A. Forstner, *J. Am. Chem. Soc.*, 1960, **82**, 5509–5510.
32 R. Goetze, H. Nöth and D. S. Payne, *Chem. Ber.*, 1972, **105**, 2637–2653.
33 M. F. Abdollahi, E. N. Welsh, M. Shayan, A. Olivier, N. Wilson-Faubert, U. Werner-Zwanziger, A. Nazemi, A. Laventure and S. S. Chitnis, *J. Am. Chem. Soc.*, 2025, **147**, 9229–9241.
34 M. A. Land, J. Ren, N. J. Roberts, K. L. Bamford, M. Shayan, A. Kutulska, T. George, J. D. Masuda and S. S. Chitnis, *Chem.– Asian J.*, 2023, **18**, e202300561.
35 Y. X. Shi, K. Xu, J. K. Clegg, R. Ganguly, H. Hirao, T. Friščić and F. García, *Angew. Chem., Int. Ed.*, 2016, **55**, 12736–12740.
36 J. Bedard, T. G. Linford-Wood, B. C. Thompson, U. Werner-Zwanziger, K. M. Marczenko, R. A. Musgrave and S. S. Chitnis, *J. Am. Chem. Soc.*, 2023, **145**, 7569–7579.
37 J. Bedard, N. J. Roberts, M. Shayan, K. L. Bamford, U. Werner-Zwanziger, K. M. Marczenko and S. S. Chitnis, *Angew. Chem., Int. Ed.*, 2022, **61**, e202204851.
38 G. V. Oshovsky, M. Zablocka, C. Duhayon, J.-P. Majoral and A.-M. Caminade, *Z. Anorg. Allg. Chem.*, 2017, **643**, 903–908.
39 M. A. Land, J. Bedard, T. George, J. D. Masuda and S. S. Chitnis, *Angew. Chem., Int. Ed.*, 2025, **64**, e202503568.
40 M. Shayan, M. F. Abdollahi, M. C. Lawrence, E. C. Guinand, M. Goulet, T. George, J. D. Masuda, M. J. Katz, A. Laventure, U. Werner-Zwanziger and S. S. Chitnis, *Chem. Commun.*, 2024, **60**, 2629–2632.
41 H. Nöth and R. Ullmann, *Chem. Ber.*, 1974, **107**, 1019–1027.
42 We acknowledge Dr Tanner George for obtaining this data and some valuable revisions to the manuscript.
43 T. Lu and F. Chen, *J. Comput. Chem.*, 2012, **33**, 580–592.
44 R. D. Kroshefsky and J. G. Verkade, *Phosphorus, Sulfur Silicon Relat. Elem.*, 1979, **6**, 391–395.
45 A. Savin, R. Nesper, S. Wengert and T. F. Fässler, *Angew. Chem., Int. Ed.*, 1997, **36**, 1808–1832.
46 P. R. Khoury, J. D. Goddard and W. Tam, *Tetrahedron*, 2004, **60**, 8103–8112.
47 K. B. Wiberg, *Angew. Chem., Int. Ed.*, 1986, **25**, 312–322.
48 (*a*) CCDC 2331623: Experimental Crystal Structure Determination, 2025, DOI: **10.5517/ccdc.csd.cc2j87nq**; (*b*) CCDC 2477097: Experimental Crystal Structure Determination, 2025, DOI: **10.5517/ccdc.csd.cc2p4mcv**; (*c*) CCDC 2477098: Experimental Crystal Structure Determination, 2025, DOI: **10.5517/ccdc.csd.cc2p4mdw**; (*d*) CCDC 2477099: Experimental Crystal Structure Determination, 2025, DOI: **10.5517/ccdc.csd.cc2p4mfx**.